International Conference on Applied Energy 2019
Aug 12-15, 2019, Västerås, Sweden
Paper ID: 0604

UNDERSTANDING THE ELECTROCHEMICAL/THERMAL PERFORMANCE OF A LARGE-FORMAT LI-ION POUCH CELL VIA A SCALING ANALYSIS APPROACH

Jie Lin[1], Howie N. Chu[1], Charles W. Monroe[1], David Howey [1*]

1 Department of Engineering Science, University of Oxford, Oxford OX1 3PJ, United Kingdom

ABSTRACT

Thermal management of large-format Li-ion cells is crucial due to their spatial- and temperature-dependent electrochemical reaction kinetics and heat generation. However, existing battery modeling mostly employs a pseudo-2D model which is not able to capture the local current density and temperature across the entire cell geometry. Therefore, in this paper, we propose a simplified 3D electrochemical/thermal model to investigate the temperature and voltage responses of a Li-ion pouch cell. Concurrently, a lock-in thermography experiment is conducted. The model can achieve good accuracy in predicting the surface temperature and cell voltage of the battery during cycling. A scaling analysis is subsequently carried out to determine the dimensionless numbers that affect the battery performance. The proposed approach helps to facilitate a fundamental understanding of the dominant mechanisms related to voltage polarization, heat generation and temperature non-uniformity.

Keywords: energy storage, Li-ion battery, electrochemistry, thermodynamics.

NONMENCLATURE

Abbreviations	
SOC	State-of-charge
OCV	Open circuit voltage
Symbols	
a_v	Surface area per volume, 1/m
b_u	Slope of OCV curve
Bi	Biot number
C_p	Heat capacity, J/(m^3·K)
F	Faraday constant, 96485 C/mol
h	Heat transfer coefficient, W/(m^2·K)
i	Current density, A/m^2
k	Thermal conductivity, W/(m^3·K)
L	Length, m
n	Number of electrons
q	State-of-charge
Q	Charge density, C/m^3
R	Universal gas constant, 8.314 J/(mol·K)
t	Time, s
T	Temperature, K
W	Width, m
δ	Thickness, m
ϕ	Electric potential, V
σ	Electrical conductivity, S/m
ρ	Electrical resistivity, Ω·m
π	Dimensionless number
Subscripts	
0	Initial state
app	Applied
cc	Current collector
s	Solid phase
l	Liquid phase
k	Kinetic

1. INTRODUCTION

Battery energy storage is crucial for the deployment of hybrid electric vehicles (HEVs) and electric vehicles (EVs) [1]. The advantages of high voltage, high energy density and low self-discharge of Li-ion batteries have made themselves an ideal candidate. However, there are challenges in operating batteries in high performance applications. In particular, high temperature and temperature inhomogeneity are commonly observed in large-format Li-ion cells which can lead to locally irregular degradation of active electrode materials, or even catastrophic thermal runaway.

Therefore, proper thermal management of Li-ion batteries is crucial [2, 3]. This requires a thorough understanding of the heat generation and dissipation rates within a cell during charging/discharging. In this regard, it is important to develop an electrochemical/thermal battery model which helps to predict thermal response and optimize operational parameters.

In battery modeling, the most commonly used electrochemical model is the standard 'pseudo-2D' (P2D) model originally developed by John Newman's group [4-6], which has been extensively adopted and coupled with different levels of thermal model. However, the P2D model is not able to capture spatially non-uniform in-plane electrochemical reactions, and most existing battery models do not consider local heat generation in the entire 3D geometry of a cell.

Therefore, in this study, we demonstrate a simplified 3D electrochemical/thermal model for large format Li-ion prismatic pouch cells which achieves computational efficiency by reducing the P2D model to a simpler structure [7]. The model is fast enough for performance prediction and thermal management while still retaining physical information that can be ascribed to microscopic charge and mass transport phenomena. A scaling analysis is carried out via non-dimensionalization of the cell model. Several key dimensionless numbers are shown to govern the dynamic performance of the battery during charging and discharging. The complexity of the model, such as the number of cell layers and mesh scheme, can be reduced by asymptotic analysis to make the model more time-efficient. The non-uniformity of both state of charge (SOC) and temperature within the cell are attributed to non-uniformity of the 3D current-density distribution. The relative importance of the fundamental dimensionless quantities in controlling local heat generation and thermal evolution will be discussed.

2. EXPERIMENTAL SETUP

A lock-in thermography test system has been set up to investigate the thermal performance of Li-ion pouch cell during charging/discharging, as shown in Fig. 1. A 20 Ah lithium iron phosphate (LFP) battery from A123 Inc. was selected for testing and parameterization.

In the experiments, the battery was held vertically with its top edge fixed into a cell holder. Other battery surfaces were freely exposed to the ambient to prevent any potential thermal contact. The positive and negative current tabs designed at the top edge of the battery were compressed onto two large copper bars to minimize the contact resistance. The copper bars were then connected to a battery tester.

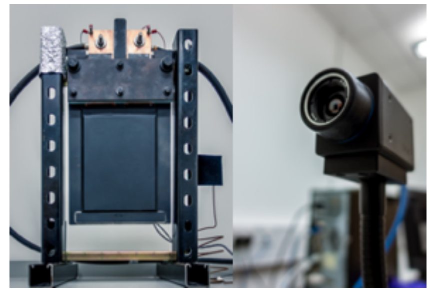

Fig 1 Lock-in thermography of a 20Ah Li-ion pouch cell

As most of the fundamental battery properties are dependent on state-of-charge (SOC), it is beneficial to cycle the battery at a certain SOC with AC current. Therefore, the applied current to the battery was set to be a square wave with identical time duration and current for charging and discharging. During cycling, the temperature response of the battery front surface was monitored and recorded via an infrared camera (FLIR A35sc). In addition, all the battery surfaces were coated with black paint to improve surface uniformity and temperature readability. An individual thermocouple was placed near the cell holder to measure the ambient temperature and calibrate the thermal camera.

3. MATHEMATICAL MODELING

3.1 A simplified electrochemical/thermal model

In order to reduce the computational complexity while maintaining the dominant characteristics of the battery, a simplified 3-D electrochemical-thermal model of a Li-ion battery is proposed. The model establishes the governing equations for the entire 3-D cell geometry, considering the charge and energy balances in the electrodes and current collectors, as summarized below.

(1) Electrodes (cathode, anode)

Charge balance in electrode: $$\nabla \cdot \vec{i}_s = -a_v i_n \qquad (1)$$

Charge balance in electrolyte: $$\nabla \cdot \vec{i}_l = a_v i_n \qquad (2)$$

Where $\vec{i}_s = -\sigma_s^{eff} \nabla \phi_s, \vec{i}_l = -\sigma_l^{eff} \nabla \phi_l$

Local SOC: $$\frac{\partial q}{\partial t} = \frac{a_v i_n}{Q_{\max}} \qquad (3)$$

Energy balance:

$$C_p^{eff}\frac{\partial T}{\partial t}=\nabla\cdot(k^{eff}\nabla T)+\sigma_s^{eff}\nabla\phi_s\cdot\nabla\phi_s+\sigma_l^{eff}\nabla\phi_l\cdot\nabla\phi_l+\rho_k i_n^2-\frac{a_v T\Delta S}{nF}i_n \tag{4}$$

Where $\rho_k=\dfrac{a_v RT}{i_0 nF},\sigma_k=\dfrac{i_0 nF}{a_v RT}$.

Reaction kinetics: $$i_n=\frac{i_0 nF}{RT}(\phi_s-\phi_l-U_{OCV}) \tag{5}$$

$$U_{OCV}=U_0+b_u q \tag{6}$$

(2) Current collectors (positive, negative)

Charge balance: $$\nabla\cdot\vec{i}_s=0 \tag{7}$$

Energy balance:

$$C_{p,cc}^{eff}\frac{\partial T}{\partial t}=\nabla\cdot(k_{cc}^{eff}\nabla T)+\sigma_{s,cc}^{eff}\nabla\phi_s\cdot\nabla\phi_s \tag{8}$$

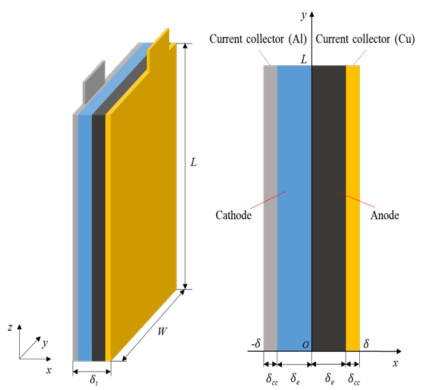

Fig 2 Model geometry Li-ion pouch cell

3.2 Dimensionless model

A scaling analysis was carried out to convert the proposed model into a dimensionless form. Proper scaling factors were determined to bound the independent and dependent variables between 0 and 1. Accordingly, the parameters appearing in the model equations were rearranged into dimensionless numbers which govern the dynamic performance of the battery during charging/discharging, such as Fourier number, Biot number, etc. The definitions of the dimensionless variables and numbers are given below.

(1) Independent and dependent variables

$$x^*=\frac{x}{\delta},y^*=\frac{y}{W},z^*=\frac{z}{L},t^*=\frac{k^{eff}t}{C_p^{eff}L^2} \tag{9}$$

$$\phi^*=\frac{nF\phi}{RT_0},T_0^*=\frac{T}{T_0},B_u=\frac{nFb_u}{RT_0},\eta^*=\phi_s^*-\phi_l^*-B_u q \tag{10}$$

(2) Dimensionless numbers

$$\pi_k=a_v^2\delta^2\frac{\sigma_k}{\sigma_s^{eff}+\sigma_l^{eff}},\pi_\sigma=\frac{\sigma_s^{eff}}{\sigma_s^{eff}+\sigma_l^{eff}} \tag{11}$$

$$\pi_Q=\frac{Q_{\max}R}{nFC_p^{eff}},\pi_i=\frac{a_v i_0 RL^2}{k^{eff}nF},\pi_S=\frac{\Delta S}{R} \tag{12}$$

$$\pi_I=\frac{i_{app}}{i_0 a_v\delta},\ Bi=\frac{h\delta}{k^{eff}} \tag{13}$$

Consequently, the dimensionless governing equations are expressed as follows.

(1) Electrodes (cathode, anode)

Charge balance in electrode:

$$\frac{\partial^2\phi_s^*}{\partial x^{*2}}+\frac{\delta^2}{W^2}\frac{\partial^2\phi_s^*}{\partial y^{*2}}+\frac{\delta^2}{L^2}\frac{\partial^2\phi_s^*}{\partial z^{*2}}=\frac{\pi_k}{\pi_\sigma}\eta^* \tag{14}$$

Charge balance in electrolyte:

$$\frac{\partial^2\phi_l^*}{\partial x^{*2}}+\frac{\delta^2}{W^2}\frac{\partial^2\phi_l^*}{\partial y^{*2}}+\frac{\delta^2}{L^2}\frac{\partial^2\phi_l^*}{\partial z^{*2}}=-\frac{\pi_k}{1-\pi_\sigma}\eta^* \tag{15}$$

SOC: $$\frac{\partial q}{\partial t^*}=\frac{\pi_i}{\pi_Q}\frac{\eta^*}{T^*} \tag{16}$$

Energy balance:

$$\frac{\partial T^*}{\partial t^*}=\left(\frac{L^2}{\delta^2}\frac{\partial^2 T^*}{\partial x^{*2}}+\frac{L^2}{W^2}\frac{\partial^2 T^*}{\partial y^{*2}}+\frac{\partial^2 T^*}{\partial z^{*2}}\right)+\frac{\pi_i\pi_\sigma}{\pi_k}\frac{1}{T^*}\left[\left(\frac{\partial\phi_s^*}{\partial x^*}\right)^2+\frac{\delta^2}{W^2}\left(\frac{\partial\phi_s^*}{\partial y^*}\right)^2+\frac{\delta^2}{L^2}\left(\frac{\partial\phi_s^*}{\partial z^*}\right)^2\right]$$
$$+\frac{\pi_i(1-\pi_\sigma)}{\pi_k}\frac{1}{T^*}\left[\left(\frac{\partial\phi_l^*}{\partial x^*}\right)^2+\frac{\delta^2}{W^2}\left(\frac{\partial\phi_l^*}{\partial y^*}\right)^2+\frac{\delta^2}{L^2}\left(\frac{\partial\phi_l^*}{\partial z^*}\right)^2\right]+\pi_i\frac{\eta^{*2}}{T^*}-\pi_i\pi_S\eta^* \tag{17}$$

(2) Current collectors (positive, negative)

Charge balance: $$\frac{\partial^2\phi_s^*}{\partial x^{*2}}+\frac{\delta^2}{W^2}\frac{\partial^2\phi_s^*}{\partial y^{*2}}+\frac{\delta^2}{L^2}\frac{\partial^2\phi_s^*}{\partial z^{*2}}=0 \tag{18}$$

Energy balance:

$$\frac{\partial T^*}{\partial t^*}=\frac{C_p^{eff}}{C_{p,cc}^{eff}}\frac{k_{cc}^{eff}}{k^{eff}}\left(\frac{L^2}{\delta^2}\frac{\partial^2 T^*}{\partial x^{*2}}+\frac{L^2}{W^2}\frac{\partial^2 T^*}{\partial y^{*2}}+\frac{\partial^2 T^*}{\partial z^{*2}}\right)+\frac{\sigma_{s,cc}^{eff}}{\sigma_s^{eff}}\frac{C_p^{eff}}{C_{p,cc}^{eff}}\frac{\pi_i\pi_\sigma}{\pi_k}\frac{1}{T^*}\left[\left(\frac{\partial\phi_s^*}{\partial x^*}\right)^2+\frac{\delta^2}{W^2}\left(\frac{\partial\phi_s^*}{\partial y^*}\right)^2+\frac{\delta^2}{L^2}\left(\frac{\partial\phi_s^*}{\partial z^*}\right)^2\right] \tag{19}$$

Therefore, the objective (dependent) variables of the model, are related to all the dimensionless numbers observed in the dimensionless model.

$$Y^*\sim\frac{\delta}{W},\frac{\delta}{L},\pi_k,\pi_\sigma,\pi_Q,\pi_i,\pi_S,\pi_I,B_u,Bi,\frac{\sigma_s^{eff}}{\sigma_{s,cc}^{eff}},\frac{C_p^{eff}}{C_{p,cc}^{eff}},\frac{k^{eff}}{k_{cc}^{eff}} \tag{20}$$

4. RESULTS AND DISCUSSION

A set of temperature and voltage responses of the battery during cycling is plotted in Fig 3 [8]. The applied current was at 4C with a cycle time of 100 s. Three surface temperature values, i.e., maximum, average and minimum, are provided in the figure. Owing to irreversible heating (ohmic and polarization heat) during charging and discharging, it was observed that the temperatures generally increased as time evolved. However, the temperatures also fluctuated around a baseline due to the existence of reversible heating (entropy heat). The entropy heat was found to be negative while charging, leading to heat absorption which slightly reduced battery temperature. On the contrary, more heat was generated during discharging which further raised the battery temperature.

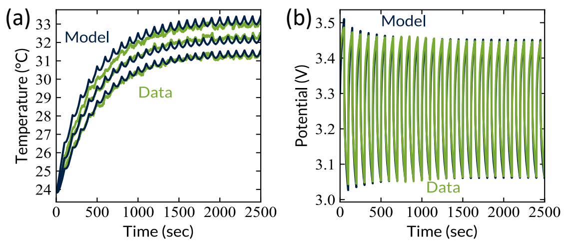

Fig 3 Temperature and voltage responses of the Li-ion pouch cell [8]

It should also be noted that simulation results from the battery model agreed well with the experimental data. Therefore, it can be employed for a detailed scaling analysis. The objective variables of this study capture the characteristics of temperature and voltage responses during cycling, as shown in Fig 4, such as voltage polarization/relaxation, heat generation and temperature uniformity.

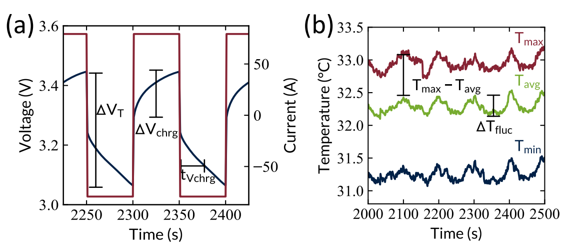

Fig 4 Objective variables in the voltage and temperature responses.

It turns out that the voltage polarization (ΔV_T and ΔV_{chrg}) is mainly affected by π_k, π_l, π_Q, π_i, B_u, Bi and $\sigma_s^{eff}/\sigma_{s,cc}^{eff}$, while the heat generation is dominated by π_k, π_l, π_Q, π_i, π_S, K_u and $\sigma_s^{eff}/\sigma_{s,cc}^{eff}$. Besides, the temperature uniformity is determined by π_k, π_l, π_i, Bi and $\sigma_s^{eff}/\sigma_{s,cc}^{eff}$.

5. CONCLUSIONS

A scaling analysis of the Li-ion pouch cell is carried out in this paper. Key dimensionless numbers that affect the temperature and voltage responses of the battery are determined to be δ/W, δ/L, π_k, π_σ, π_Q, π_i, π_S, π_l, B_u and $\sigma_s^{eff}/\sigma_{s,cc}^{eff}$. These parameters significantly affect the voltage and temperature responses of the battery during charging and discharging, as well as temperature uniformity.

ACKNOWLEDGEMENT

The authors gratefully acknowledge funding from the EPSRC Translational Energy Storage Diagnostics (TRENDs) project (ref EP/R020973/1).

REFERENCE

[1] Schuster E, Ziebert C, Melcher A, Rohde M, Seifert HJ. Thermal behavior and electrochemical heat generation in a commercial 40 Ah lithium ion pouch cell. J Power Sources. 2015;286:580-9.

[2] Belt JR, Ho CD, Miller TJ, Habib MA, Duong TQJJops. The effect of temperature on capacity and power in cycled lithium ion batteries. 2005;142:354-60.

[3] Amine K, Liu J, Belharouak IJEc. High-temperature storage and cycling of C-LiFePO4/graphite Li-ion cells. 2005;7:669-73.

[4] Fuller TF, Doyle M, Newman JJJotES. Simulation and optimization of the dual lithium ion insertion cell. 1994;141:1-10.

[5] Fuller TF, Doyle M, Newman JJJotES. Relaxation phenomena in lithium ‐ ion ‐ insertion cells. 1994;141:982-90.

[6] Doyle M, Fuller TF, Newman JJJotES. Modeling of galvanostatic charge and discharge of the lithium/polymer/insertion cell. 1993;140:1526-33.

[7] Newman JS, Tobias CWJJoTES. Theoretical analysis of current distribution in porous electrodes. 1962;109:1183-91.

[8] Chu HN, Monroe CW. Characterizing Lithium-Ion Cell State with a Streamlined Electrochemical/Thermal Model Parameterized By Lock-in Thermography. Meeting Abstracts. 2018;MA2018-02:211-211.